Contrib Mineral Petrol (2005) 150: 119–130
DOI 10.1007/s00410-005-0013-z

ORIGINAL PAPER

Chusi Li · Edward M. Ripley · Arindam Sarkar
Dongbok Shin · Wolfgang D. Maier

Origin of phlogopite-orthopyroxene inclusions in chromites from the Merensky Reef of the Bushveld Complex, South Africa

Received: 22 March 2005 / Accepted: 6 June 2005 /

Abstract About 30% of the chromite grains of variable sizes in a chromitite seam at the base of the Merensky Reef of the Bushveld Complex on the farm Vlakfontein contain abundant composite mineral inclusions. The inclusions are polygonal to circular with radial cracks that protrude into the enclosing chromite. They vary from a few microns to several millimeters in diameter and are concentrated in the cores and mantles of chromite crystals. Electron backscattered patterns indicate that the host chromites are single crystals and not amalgamations of multiple grains. Na-phlogopite and orthopyroxene are most abundant in the inclusions. Edenitic hornblende, K-phlogopite, oligoclase and quartz are less abundant. Cl-rich apatite, rutile, zircon and chalcopyrite are present at trace levels. Na-phlogopite is unique to the inclusions; it has not been found elsewhere in the Bushveld Complex. Other minerals in the inclusions are also present in the matrix of the chromitite seam, but their compositions are different. The $Mg/(Mg+Fe^{2+})$ ratios of orthopyroxene in the inclusions are slightly higher than those of orthopyroxene in the matrix. K-phlogopite in the inclusions contains more Na than in the matrix. The average compositions of the inclusions are characterized by high MgO (26 wt%), Na_2O (2.4 wt%) and H_2O (2.6 wt%), and low CaO (1.1 wt%) and FeO (4.4 wt%). The $\delta^{18}O$ value of the trapped melt, estimated by analysis of inclusion-rich and inclusion-poor chromites, is ~7‰. This value is consistent with the previous estimates for the Bushveld magma and with the $\delta^{18}O$ values of silicate minerals throughout the reef. The textural features and peculiar chemical compositions are consistent with entrapment of orthopyroxene with variable amounts of volatile-rich melts during chromite crystallization. The volatile-rich melts are thought to have resulted from variable degrees of mixing between the magma on the floor of the chamber and Na-K-rich fluids expelled from the underlying crystal pile. The addition of fluid to the magma is thought to have caused dissolution of orthpyroxene, leaving the system saturated only in chromite. Both oxygen and hydrogen isotopic values are consistent with the involvement of a magmatic fluid in the process of fluid addition and orthopyroxene dissolution. Most of the Cr and Al in the inclusions was contributed through wall dissolution of the host chromite. Dissolution of minor rutile trapped along with orthopyroxene provided most of the Ti in the inclusions. The Na- and K-rich hydrous silicate minerals in the inclusions were formed during cooling by reaction between pyroxene and the trapped volatile-rich melts.

Communicated by T.L. Grove

C. Li (✉) · E. M. Ripley · A. Sarkar
Department of Geological Sciences,
Indiana University, Bloomington, IN 47405, USA
E-mail: cli@indiana.edu
Tel.: +1-812-8551558
Fax: +1-812-8557899

D. Shin
Korea Institute of Geoscience and Mineral Resources,
Daejeon, 305-350, South Korea

W. D. Maier
Sciences de la Terre, Université du Québec à Chicoutimi,
Chicoutimi, G7H 2B1 Québec, Canada

Introduction

The presence of silicate inclusions in the chromitite layers in the Bushveld Complex, including the famous Merensky Reef, has been known for several decades (McDonald 1965; Legg 1969; Cameron 1979; Hulbert and von Gruenewaldt 1985; Barnes and Maier 2002). However, details regarding the mineralogy, textural features and isotopic compositions of the inclusions are poorly known. This paper focuses on the morphology, mineralogy and chemical and stable isotopic compositions of abundant composite silicate inclusions that are present in the basal chromitite seam of the Merensky

Reef at Impala Platinum Mine on the farm Vlakfontein. Compositions of minerals that occur interstitially in the chromitite seam, in footwall anorthosite and in hangingwall norite are also provided as they place constraints on the origin of the inclusions and their chromite hosts.

Geological background

The Bushveld Complex is a layered mafic-ultramafic intrusion situated in northern South Africa with a surface exposure over an area of 240×350 km (Fig. 1). The complex is subdivided into five zones from bottom to top (Hall 1932; Eales and Cawthorn 1996; Cawthorn et al. 2002): the Marginal Zone (gabbro-norite), the Lower Zone (peridotites and orthopyroxenites), the Critical Zone (orthopyroxenites and chromitites), Main Zone (gabbro-norites) and Upper Zone (anorthosites, diorites and magnetitites).

The Bushveld Complex hosts the world's largest platinum-group element (PGE) deposits. The PGE mineralization of the Bushveld Complex mainly occurs in stratiform sulfide-bearing layers, most importantly the Merensky Reef (Lee 1983) and sulfide-poor chromitite layers, most importantly the UG2 (Hiemstra 1986) at the top of the Upper Critical Zone. The UG2 chromitite layer and the Merensky Reef are generally less than 1.5 m in thickness and extend laterally over most parts of the complex.

The lithological characteristics of the Merensky Reef in the western lobe of the complex have been described in detail by Barnes and Maier (2002), Leeb-du Toit (1986), and Viljoen and Hieber (1986). In most of the western lobe of the Bushveld Complex, up to 3 vol% disseminated sulfides (pyrrhotite + pentlandite + chalcopyrite ± pyrite) are found in an interval consisting of anorthosite or leuconorite, overlain by a chromitite seam (commonly 1–3 cm in thickness), pegmatoidal pyroxenite, a second thin chromitite seam, and a 3–6 m medium- to coarse-grained pyroxenite. The sulfides are most commonly associated with the two chromitite seams and the pegmatoid, but may also occur up to several centimeters into the anorthosite footwall. Average Pt + Pd tenors in the Merensky Reef are up to 9 ppm. The concentrations of PGE are generally correlated with S content in the rocks (Barnes and Maier 2002). Platinum-group minerals are dominated by sulfides, bismuthotellurides and arsenides (Kingston and El-Dosuky 1982; Mostert et al. 1982; Prichard et al. 2004). They occur most commonly within base metal sulfide assemblages and less commonly in the alteration aureoles of base metal sulfides (Li et al. 2004).

The core used in this study is from the Merensky Reef at Impala Platinum Mine on the farm Vlakfontein, which differs from the description given above in that the upper chromitite seam is missing here and medium-grained melanorite occurs in place of pegmatoidal pyroxenite (Fig. 2). The lower 30 cm of the analysed core interval is footwall anorthosite. The contact with the overlying chromitite seam is sharp and curved. The chromitite seam is −3 cm in thickness. In the following we will refer to the anorthosite underlying the chromitite seam as footwall and the overlying melanorite as hangingwall. The chromitite seam contains ~70% chromite, ~15% plagioclase and 10% orthopyroxene. The hangingwall melanorite contains

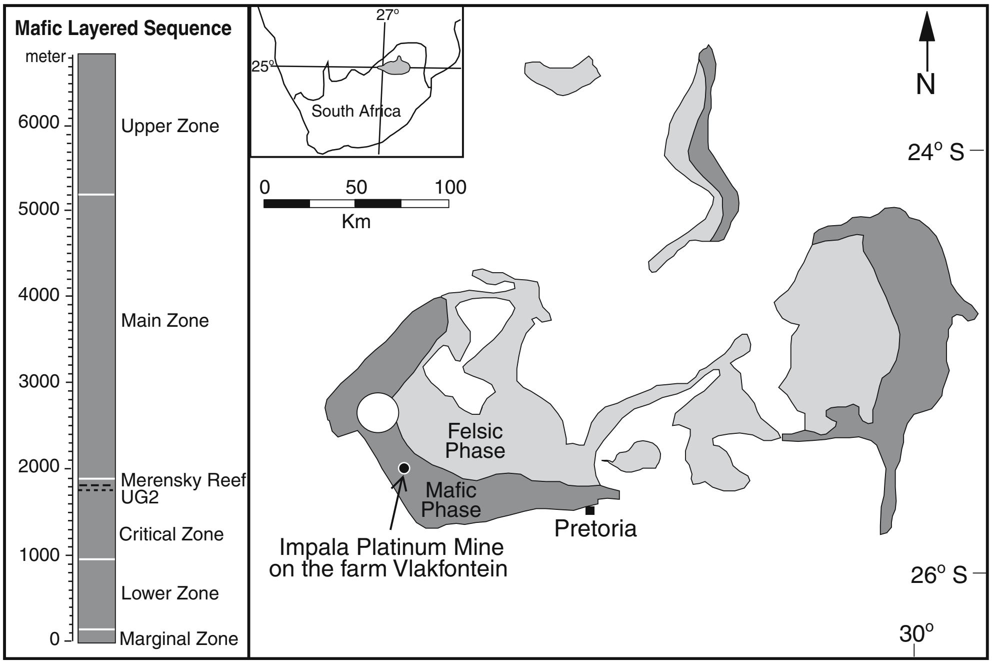

Fig. 1 Simplified surface geologic map of the Bushveld Complex, with a lithologic column showing the stratigraphic position of the Merensky Reef. The samples used in this study are from the Impala Platinum Mine on the farm Vlakfortein

Fig. 2 Photograph of a half core through the Merensky Reef on the farm Vlakfortein

~75% granular orthopyroxene and ~25% poikilitic plagioclase. Minor amounts of sulfides and trace amounts of phlogopite, quartz, apatite, zircon and magnetite are disseminated throughout the core. Alteration assemblages of epidote and actinolite in the contact between primary silicates and sulfides or chromite that are common elsewhere (Li et al. 2004) are extremely rare in this core. Only minor talc alteration is present in the microfractures of some orthopyroxene crystals in the samples.

Analytical methods

Detailed textural analyses were conducted using backscattered electron (BSE) images obtained from the CAMECA SX50 electron microprobe at Indiana University. Estimates of mineral proportions in inclusions in chromites were made using BSE images and GIS area-volume software.

The textures of individual chromite grains were investigated using electron backscattered diffraction (EBSD) patterns (for details see Prior et al. 1999). The EBSD data were collected using a Quanta FEG 400F scanning electron microscope fitted with an EBSD detector (NORDLYS II) from HKL technology. The data were then analyzed using the Channel v5.0 software from HKL technology.

Mineral chemical compositions were determined via electron microprobe by wavelength-dispersive X-ray analysis at 15 kV, 20 nA of beam current and a counting time of 20 s. Beam sizes of 1 and 2 μm in diameter were used for anhydrous and hydrous minerals, respectively. Potential fluorescence interference for silicate inclusions from the host chromite was checked using plagioclase and quartz of inclusions. The accuracy of the analyses was monitored using reference materials of similar compositions.

Oxygen from silicates and chromites was extracted using the BrF_5 method of Clayton and Mayeda (1963). Oxygen was converted to CO_2 by reaction with a heated graphite disk. Isotopic analyses were made using a Finnigan MAT 252 stable isotope ratio mass spectrometer, with results reported in standard delta notation relative to V-SMOW. Analytical uncertainty was less than 0.05‰, and sample reproducibility was ±0.1 to ±0.2‰. The value of NBS-28 quartz in our lab is 9.6 ± 0.2‰.

Samples for hydrogen isotopic analyses were analyzed using a high-temperature-EA-continuous flow method similar to that reported by Sharp et al. (2001). Samples were loaded into silver cups and combusted at 1,400°C in a glassy carbon column. Hydrogen was analyzed using a Finnigan Delta Plus-XP stable isotope ratio mass spectrometer. Several standards were run with each series of analyses. NBS-30 biotite was taken as −65‰. Laboratory mineral standards range from −60 to −100‰. Results are reported in delta notation with respect to V-SMOW. Analytical reproducibility was within ±0.2‰ and sample reproducibility was ±2‰.

Results

Distribution and morphology of inclusions

Chromite crystals in the basal chromitite layer of the Merensky Reef at Impala Platinum Mine on the farm Vlakfontein contain three types of mineral inclusions; (1) abundant composite mineral inclusions, (2) minor solitary rutile inclusions and (3) rare solitary plagioclase inclusions. The composite mineral inclusions are present in more than 30% of chromite crystals of variable sizes in the chromitite seam. Solitary rutile and plagioclase inclusions occur with composite mineral inclusions in the same chromite crystals as well as in separate chromite crystals.

Solitary plagioclase inclusions are commonly >2 mm in diameter and have characteristic tabular or elongated shapes. They tend to occur in the margins of relatively large, irregular chromite crystals. Some solitary plagioclase inclusions are parts of large, poikilitic plagioclase that wraps around the host chromite (Fig. 3a).

The composite mineral inclusions in the basal chromitite seam of the Merensky Reef exhibit characteristic polygonal to circular shapes (Fig. 3b–e). They vary from a few microns to several millimeters in diameter and are concentrated most commonly in the cores (Fig. 3b–d) and less commonly in the mantle (Fig. 3e) of chromite

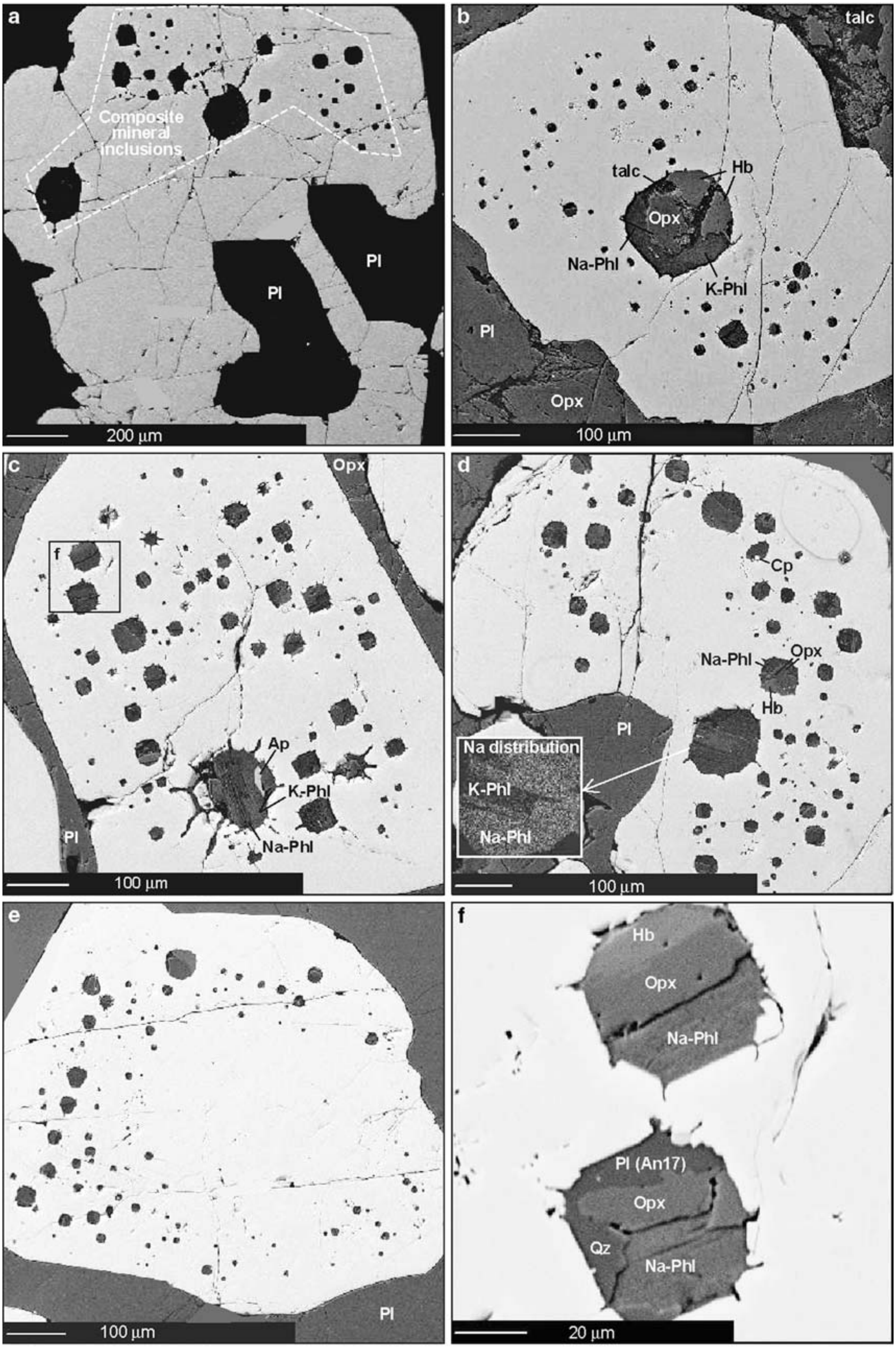

Fig. 3 Back scattered electron (*BSE*) images showing the textures and mineral assemblages of inclusions in chromites in the Merensky Reef on the farm Vlakfortein. *Hb* hornblende, *Ap* apatite, *Cp* chalcopyrite, *K-Phl* potassium phlogopite, *Na-Phl* sodium phlogopite, *Opx* orthopyroxene, *Pl* plagioclase, *Qz* Quartz

crystals regardless of the sizes and shapes of the chromite hosts. Na-phlogopite (Na > K) and orthopyroxene are most abundant in the composite mineral inclusions; hornblende, K-phlogopite (K > Na), oligoclase and quartz are less abundant; and apatite, rutile, zircon and chalcopyrite are present only at trace levels. Minor talc alteration occurs in microfractures cutting through the inclusions (Fig. 3b).

The orientation of individual crystals in the composite mineral inclusions is random with respect to the host chromites (Fig. 3b–d). The grain sizes of the minerals tend to increase with the sizes of inclusions. K-phlogopite commonly occurs along with Na-phlogopite, either side by side (Fig. 3b) or partially wrapping around each other (Fig. 3c, d). In either case the contact between these two phases is marked by an abrupt change in Na concentration (see inset in Fig. 3d). Reactions between orthopyroxene and the melts from which hornblende and phlogopite crystallized are indicated based on the irregular contacts between orthopyroxene and the hydrous silicates (Fig. 3f). With almost no exception the inclusions, including their radial cracks, are completely filled by silicate minerals (Fig. 3f). EBSD patterns reveal that the inclusion-bearing chromites, such as those shown in Fig. 3b–e, are single crystals and not amalgamations of multiple grains.

Similar inclusions have been reported from the Western Laouni mafic intrusion in Algeria (Lorand and Cottin 1987), the Oman ophiolite (Lorand and Ceuleneer 1989), the dunite pipes of the Bushveld Complex (Stumpfl and Rucklidge 1982) and the J-M Reef of the Stillwater Complex (Barnes SJ unpublished data; Boudreau et al. 1986; Boudreau 1988).

Compositional variations of inclusions, chromite, and related minerals

In the following we will focus on the composite mineral inclusions. The average compositions of minerals in the inclusions and the host chromites are listed in Table 1. The compositions of K-phlogopite and orthopyroxene from the matrix of the chromitite seam and the footwall anorthosite and hanginging melanorite are also listed for comparison. Important compositional variations of individual minerals of different occurrences are summarized below.

No chemical zoning is seen in the inclusion-free chromites (Fig. 4a, b). In contrast, the inclusion-bearing chromites are chemically zoned; the inclusion-bearing zones have higher mg-number (Fig. 4a) and lower Ti and Al concentrations than the inclusion-free zones (Fig. 4b). The compositions of inclusion-free zones of inclusion-bearing chromites are similar to those of inclusion-free chromites. The chemical variations in the inclusion-bearing chromites are apparently related to the presence of inclusions, indicating that post-entrapment chemical exchange between the inclusions and host chromites took place.

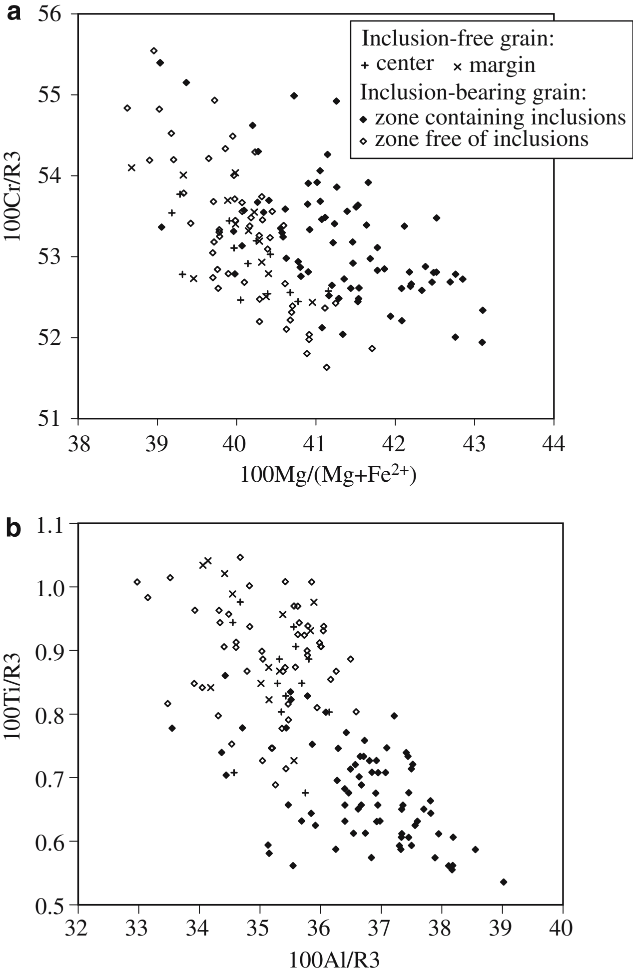

Fig. 4 Compositional variations of inclusion-free and inclusion-bearing chromites

Orthopyroxenes from the footwall anorthosite and hangingwall melanorite of the chromitite seam have rather similar mg-numbers, Cr, Al and Ti contents (Fig. 5a–c). Orthopyroxenes from the matrix of the chromitite seam are characterized by higher mg-numbers and Al concentrations (Fig. 5a, b). Orthopyroxenes in the inclusions have bimodal compositions. Some of them have mg-numbers similar to those of orthopyroxenes from the matrix and the others have higher mg-numbers (Fig. 5a). The orthopyroxenes with higher mg-numbers are also characterized by lower Al and Ti contents (Fig. 5b, c).

The Na-phlogopites and coexisting K-phlogopites in the inclusions are characterized by high Cr concentrations (Fig. 3a). K-phlogopites in the inclusions also contain more Na than those in the footwall, hangingwall and matirx of the chromitite seam (Fig. 6a). Na-phlogopites and K-phlogopite in the inclusions have mg-numbers similar to those of K-phlogopites in the matrix. K-phlogopites in the footwall anorthosite are characterized by low Ti concentrations. K-phlogopites in the hangingwall melanorite are distinctly more

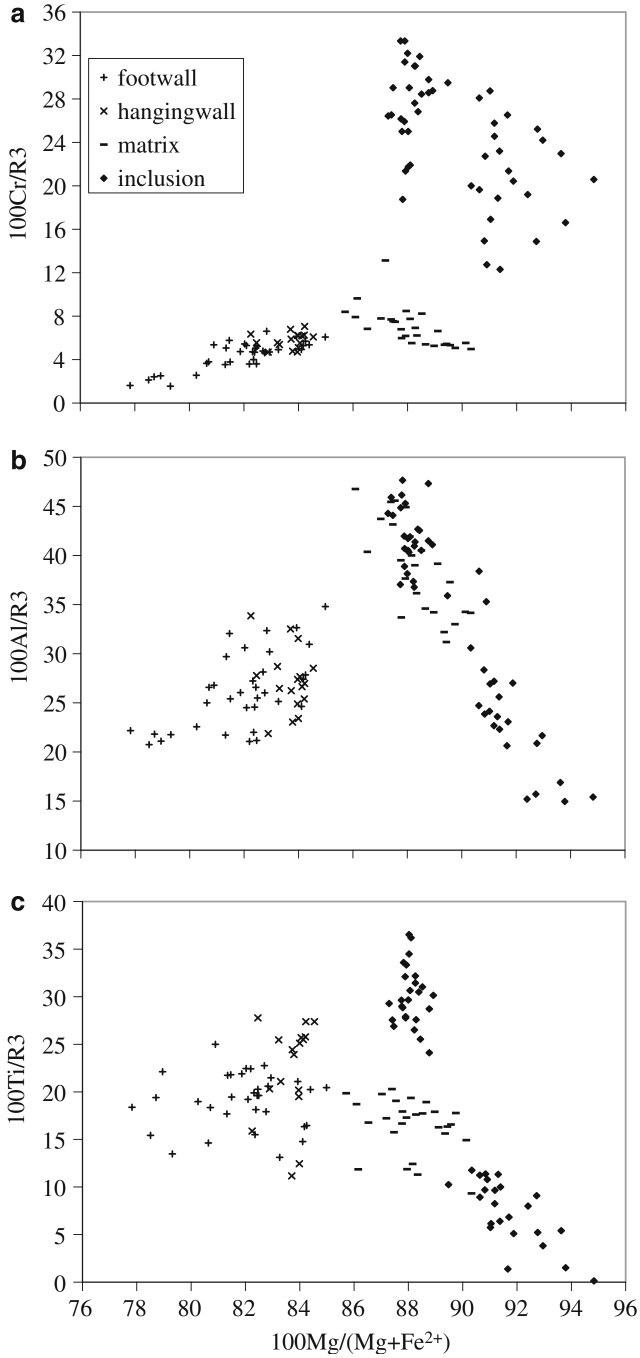

Fig. 5 Comparison of the compositions of orthopyroxene in inclusions and in the footwall and hangingwall rocks

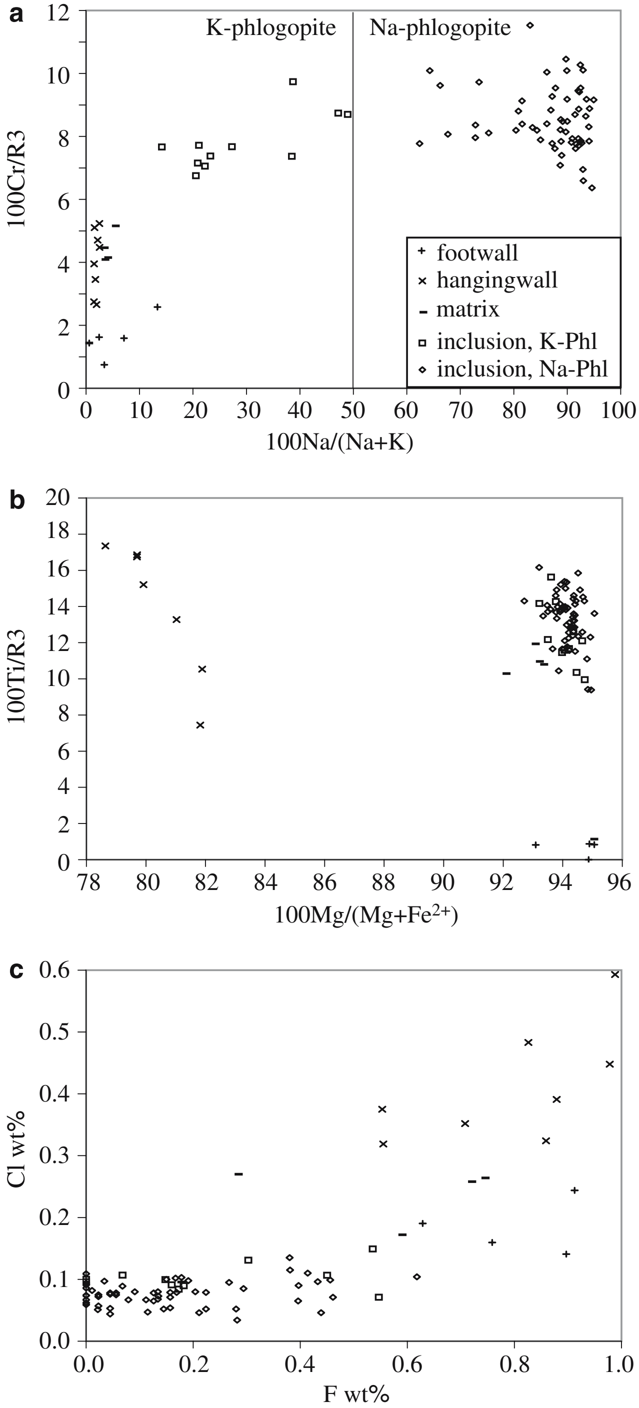

Fig. 6 Comparison of the compositions of phlogopite in inclusions and related rocks

Fe-rich (Fig. 6b). Both types of phlogopites in the inclusions contain less F and Cl than K-phlogopites in the footwall, hangingwall and matirx of the chromitite seam (Fig. 6c), which is mainly due to the higher proportions of mica present in the inclusions relative to those of surrounding rock types.

Amphibole in the inclusions is edenitic hornblende whereas interstitical amphibole in the hangingwall norite\ is actinolitic hornblende. The hornblende in the inclusions is also characterized by higher Ti, Cr and Na than the hornblende in the hangingwall norite (Table 1). Plagioclase in the inclusions is much more sodic (Ab = 75) than that in the matrix of the chromitite seam (Ab = 25). Apatite in the inclusions is characterized by high Cl (4.7 wt%) and low F (0.4 wt%), which are within the ranges of apatite from the Critical Zone (Willmore et al. 2000).

Bulk inclusion composition

A total of 23 large composite mineral inclusions free of microfractures and talc alteration were selected for volume-area analysis. The volume percentages of individual minerals in the inclusions were converted to weight percentages using the medium densities of the minerals given by Deer et al. (1992). The results are listed in Table 2. The average modal compositions of the inclusions are 41% Na-phlogopite, 32% orthopyroxene, 14% K-phlogopite and 13% hornblende. Other minor phases such as oligoclase, quartz, apatite, rutile, zircon and chalcopyrite together comprise $<2\%$ of the inclusions. The bulk compositions of the inclusions calculated using the average modal compositions and the average compositions of the minerals are given in Table 3. The bulk compositions of the inclusions are characterized by high MgO, TiO_2, Cr_2O_3, Na_2O and H_2O and low FeO and CaO.

Stable isotopic compositions

Stable isotopic data for samples from the footwall anorthosite, chromitite seam, and hangingwall melanorite are given in Table 4. $\delta^{18}O$ values of orthopyroxene, plagioclase, phlogopite, and chromite fall in reasonably narrow ranges as follow: orthopyroxene 6.1–7.3; plagioclase, 6.8–7.4; phlogopite, 5.8–6.8; chromite, 4.3–4.8‰. Chromite grains that contain a large proportion of inclusions are characterized by slightly higher $\delta^{18}O$ values of 5.4–6.1‰. A simple mass balance using a chromite $\delta^{18}O$ value of 4.6‰ suggests that the included silicate minerals are characterized by a bulk $\delta^{18}O$ value near 7‰. Plagioclase-orthopyroxene and orthopyroxene-phlogopite Δ values range from 0 to 0.2 and 0 to 0.8‰, respectively. Only one sample of orthopyroxene was collected from the chromitite seam; the observed orthopyroxene-chromite Δ value was 2.9‰. The orthopyroxene and plagioclase $\delta^{18}O$ values are slightly higher than those that are normally considered to be representative of minerals that crystallized from uncontaminated mantle-derived magmas (~5.5–6.0‰, e.g., Ito et al. 1987; Eiler 2001). The values are very similar to those obtained in larger scale studies of the Bushveld Complex by Schiffries and Rye (1989) and Harris et al. (2004). These authors concluded that the magma which produced the Bushveld Complex had experienced variable, but relatively high (up to 40%) degrees of contamination by high-^{18}O country rocks in the lower to middle crust. A bulk magma with a $\delta^{18}O$ value of 7‰ computed from the inclusions in chromite compares favorably with the value of 7.1‰ estimated by Harris et al. (2004).

One sample of inclusion-rich chromite was analyzed for hydrogen isotopic composition. The δD value of −76‰ is within the range for phlogopite-rich samples of the Merensky Reef reported by Mathez et al. (1994).

Discussion

Post-entrapment reaction and crystallization

The compositional variations between the inclusion-free and inclusion-bearing chromites (Fig. 4) indicate that the inclusion-bearing chromites lost Ti and gained Mg, possibly through subsolidus chemical exchange with the entrapped materials. The compositional variations of orthopyroxene in the inclusions (Fig. 5c) are consistent with variable degrees of exchange with host chromites. Orthopyroxene that is characterized by high Ti and low Mg may have resulted from higher degrees of such exchange.

High Cr contents of the inclusions may also have resulted from subsolidus exchange with the host chromites. However, there are no systematic variations of Cr concentrations in chromites in the samples (Fig. 4a) to support such a mechanism. It is more likely that the inclusions gained Cr through dissolution of the chromite walls. Wall dissolution of chromites could also contribute Al to the inclusions, which explains the high Al/Ca ratios in the inclusions. The silicate-filled radial cracks of the inclusions could be evidence of wall dissolution. High Ti in the edenitic hornblende and K- and Na-phlogopite in the inclusions can likewise be explained by reaction with trapped rutile crystals.

Phase relations in the $KAlSiO_2$-Mg_2SiO_4-SiO_2-H_2O system at 2 kb total pressure (Luth 1967) indicate that K-phlogopite could form from reaction between orthopyroxene and a volatile-rich melt. Carman (1974) determined that Na-phogopite could form through the reaction between olivine and a volatile rich melt in the system $NaAlSiO_2$-Mg_2SiO_4-SiO_2-H_2O. Similarly, it is possible for Na-phlogopite to form through reaction between orthopyroxene and a volatile-rich melt. The coexistence of K- and Na-phlogopite in some inclusions suggests that both reactions occurred on local scales.

The experiments of MacNeil and Edgar (1987) indicate that Na-rich amphibole could form through a reaction involving chromite, clinopyroxene and a volatile-rich melt. The presence of edenitic hornblende in some composite mineral inclusions in the chromitite seam of the Merensky Reef suggests that the trapped melt may have crystallized clinopyroxene at an early stage, but the clinopyroxene subsequently reacted with the residual liquid to form edenitic hornblende. Minor oligoclase, quartz and apatite in the inclusions possibly crystallized from the residual liquid of the trapped melt. The experiments of Mathez and Webster (2004) on apatite-melt-fluid systems indicate that Cl-rich apatite, such as that in the inclusions from the Merensky Reef, requires the presence of a brine.

Origin of the trapped melt and orthopyroxene, and host chromite

At least three mechanisms have been proposed for the origin of chromitite layers in layered intrusions. One is

Table 1 Average compositions of minerals from the Merensky Reef at Impala Platinum Mine, Farm Vlakfortein area

Mineral	Na-Phl	K-Phl	K-Phl	K-Phl	K-Phl		Orthopyroxene					Horblende			Oligoclase		Apatite		Chromite			
Type	incl	incl	mtx	fw	hw		incl	mtx	fw	hw		incl	hw		incl		incl		Cr-1	Cr-2	Cr-3	Cr-4
n	58	11	5	5	8		50	28	34	16		15	2		3		4		75	52	13	13
SiO_2	42.36	40.81	40.33	41.56	38.21	SiO_2	57.24	55.25	53.77	53.96	SiO_2	47.00	52.89	SiO_2	61.83	La_2O_3	0.40	SiO_2	0.02	0.02	0.02	0.01
TiO_2	3.95	3.21	2.45	0.47	4.03	TiO_2	0.54	0.71	0.86	1.35	TiO_2	2.20	0.45	Al_2O_3	24.59	Ce_2O_3	0.07	TiO_2	0.55	0.71	0.68	0.74
Al_2O_3	14.74	14.59	14.85	15.18	14.25	Al_2O_3	0.87	1.55	1.06	1.48	Al_2O_3	9.77	3.94	FeO	0.45	SiO_2	0.39	Al_2O_3	19.01	18.05	18.18	17.92
Cr_2O_3	2.40	2.10	0.99	0.38	1.07	Cr_2O_3	0.96	0.39	0.26	0.47	Cr_2O_3	2.08	0.76	CaO	4.87	FeO	0.27	Cr_2O_3	41.06	40.81	40.57	40.69
FeO	2.62	2.56	2.97	2.51	8.60	Fe_2O_3	1.05	2.28	3.28	3.79	FeO	4.26	5.71	Na_2O	7.67	MgO	0.02	V_2O_3	0.26	0.26	0.26	0.26
MnO	0.00	0.00	0.01	0.02	0.01	FeO	6.48	7.71	11.39	10.20	MnO	0.03	0.09	K_2O	0.01	MnO	0.01	Fe_2O_3	7.65	8.61	8.72	8.68
MgO	23.74	23.64	23.59	25.76	19.45	MnO	0.16	0.20	0.29	0.26	MgO	19.04	20.79	Total	99.42	CaO	50.91	FeO	21.85	22.27	22.24	22.25
CaO	0.09	0.06	0.03	0.02	0.02	MgO	32.29	32.06	28.91	29.31	CaO	11.09	12.18			SrO	2.05	MnO	0.00	0.00	0.00	0.00
Na_2O	4.65	1.75	0.23	0.33	0.12	CaO	0.02	0.00	0.00	0.00	Na_2O	2.07	0.45	Si	2.746	Na_2O	0.07	MgO	8.63	8.36	8.36	8.32
K_2O	1.07	6.52	9.34	8.74	9.30	NiO	0.12	0.12	0.14	0.13	K_2O	0.17	0.29	Al	1.286	P_2O_5	40.18	NiO	0.17	0.20	0.18	0.22
F	0.16	0.23	0.50	0.67	0.79	Na_2O	0.09	0.01	0.01	0.03	F	0.12	0.48	Fe	0.017	F	0.37	Total	99.19	99.29	99.21	99.09
Cl	0.08	0.10	0.21	0.17	0.41	K_2O	0.15	0.11	0.24	0.18	Cl	0.08	0.11	Ca	0.232	Cl	4.65					
H_2O	4.33	4.17	3.95	3.93	3.64	Total	99.95	100.41	100.21	101.15	H_2O	2.04	1.88	Na	0.660	H_2O	0.46	Si	0.006	0.005	0.006	0.003
Total	100.18	99.75	99.45	99.73	99.89						Total	99.96	100.02	K	0.000	Total	100.49	Al	5.810	5.549	5.588	5.522
O = F	−0.07	−0.10	−0.21	−0.28	−0.33	Si	1.985	1.930	1.924	1.908	O = F	−0.052	−0.204	ab	73.91	O = F, Cl	−1.20	Cr	8.420	8.414	8.367	8.413
O = Cl	−0.02	−0.02	−0.05	−0.04	−0.09	Al	0.036	0.064	0.045	0.062	O = Cl	−0.019	−0.024	an	26.05	Total	99.28	Fe^{3+}	1.493	1.690	1.712	1.709
Total	100.10	99.63	99.18	99.41	99.46	Cr	0.026	0.011	0.007	0.013	Total	99.89	99.79					Ti	0.107	0.140	0.134	0.145
						Fe^{3+}	0.027	0.060	0.088	0.101								V	0.054	0.055	0.054	0.054
Si	5.737	5.681	5.701	5.803	5.559	Ti	0.020	0.027	0.033	0.051	Si	6.631	7.425					Mg	3.335	3.250	3.250	3.245
Al	2.353	2.394	2.474	2.498	2.444	Mg	1.668	1.670	1.542	1.545	Al	1.625	0.652					Fe^{2+}	4.739	4.857	4.852	4.867
Ti	0.402	0.336	0.260	0.049	0.441	Fe^{2+}	0.188	0.225	0.341	0.302	Ti	0.233	0.048					Mn	0.000	0.000	0.000	0.000
Cr	0.257	0.231	0.111	0.042	0.123	Mn	0.005	0.006	0.009	0.008	Cr	0.232	0.084					Ni	0.036	0.042	0.037	0.046
Fe	0.297	0.298	0.351	0.293	1.046	Ca	0.001	0.000	0.000	0.000	Mg	4.005	4.351					Mg#	0.41	0.40	0.40	0.40
Mn	0.000	0.000	0.001	0.002	0.001	Ni	0.003	0.003	0.004	0.003	Mn	0.004	0.011					Al/R3	0.37	0.35	0.35	0.35
Mg	4.793	4.906	4.971	5.363	4.219	Na	0.006	0.001	0.001	0.002	Fe	0.503	0.670					Cr/R3	0.53	0.53	0.53	0.53
Ca	0.013	0.009	0.005	0.003	0.003	K	0.004	0.003	0.006	0.005	Ca	1.676	1.832									
Na	1.221	0.472	0.063	0.009	0.034	Mg#	0.90	0.88	0.82	0.84	Na	0.566	0.123									
K	0.185	1.158	1.684	1.557	1.726						K	0.030	0.052									

incl inclusion in chromite; *mtx* matrix of chromitite seam; *fw* footwall of chromitite seam; *hw* hangingwall of chromitite seam; *K-Phl* potasium phlogopite; *Na-Phl* sodium phlogopite; *Mg#* = $Mg/(Mg + Fe^{2+})$; *Cr-1* inclusion-bearing zone; *Cr-2* inclusion-free zone; *Cr-3* core of inclusion-free grain; *Cr-4* rim of inclusion-free grain

Table 2 Modal Composition of Inclusions

Mineral	Range (wt%)	Average (wt%)
Na-phlogopite	20–60	41
Orthopyroxene	25–55	32
K-phlogopite	0–20	14
Hornblende	0–30	13

the magma mixing process described by Irvine (1977) whereby chromite over-saturation is reached by blending of two magmas, each near or just at chromite saturation. Irvine and Sharpe (1986), utilizing mineralogic and Sr isotopic data proposed that the Merensky Reef marked the mixing interface between an ultramafic and an anorthositic magma. Irvine (1975) also proposed that contamination of a mafic magma by Si-rich material could cause chromite crystallization. Kruger et al. (2002) have also embraced such a model for the chromitite seam of the Merensky Reef. Boudreau (1988) suggested that minor chromite in the J-M Reef of the Stillwater Complex is a secondary mineral produced by the incongruent hydration melting of Cr-bearing pyroxene. Similarly, Nicholson and Mathez (1991) and Mathez et al. (1997) proposed that the chromitite seam in the Merensky Reef formed by crystallization of chromite alone from a secondary melt produced by hydration melting of pyroxenite. These authors noted that the experiments of Ford et al. (1972), Sisson and Grove (1993), and Gaetani et al. (1994) on basaltic systems indicate that the addition of H_2O decreases the liquidus temperature of silicate minerals more significantly than spinel.

The Merensky Reef has Sr and Nd isotopic compositions and incompatible element ratios that are between the values for the Lower Zone and the Main Zone (Kruger and Marsh 1982; Maier and Barnes 1998; Maier et al. 2000; Barnes and Maier 2002). This has been considered by many previous researchers to be evidence for mixing of the Lower Zone and the Main Zone magmas at the levels of the Merensky cyclic unit. The initial compositions of these two magmas are thought to be represented by the average compositions of chilled marginal rocks from the two zones and are listed in Table 3. A mixing (±contamination) model for chromite genesis in the Merensky Reef circumvents any potential mass balance problems because Cr may have been derived from a sufficiently large volume of magma, but it does not explain the inclusions found in chromite or the signs of fluid interaction described by Nicholson and Mathez (1991) and Mathez et al. (1997).

Barnes and Maier (2002) estimated that the Merensky Reef at Impala represents a 60:40 mixture between the Lower Zone magma and the Main Zone magma based on incompatible element ratios. For major elements, the effect of silicate crystallization in the chamber needs to be taken into account. The footwall of the Merensky Reef at Impala varies from lecogabbro to anorthosite, which suggests that plagioclase was a liquidus phase in the resident magma. We have used the MELTS program of Ghiorso and Sack (1995) to calculate the composition of a residual liquid derived from the initial magma of the Lower Zone after ~44% fractional crystallization when plagioclase was on the liquidus. The composition of a potential parental magma to the Merensky Reef was computed as a 50:50 mixture of the fractionated magma and a new input of the B3 magma that formed the Main Zone (Sharpe 1981; Table 3).

Variations in the crystallization sequence of this magma as a function of H_2O content were calculated using the MELTS program of Ghiorso and Sack (1995) at 2 kb and the QFM buffer, and is illustrated in Fig. 7. At low H_2O content (<0.2 wt%) plagioclase is the first phase to appear on the liquidus. At intermediate H_2O content (0.2–1.6 wt%) orthopyroxene is the first phase to appear on the liquidus, and at high H_2O content (>1.6 wt%) olivine is the first phase to appear on the liquidus. The liquidus temperatures of these phases decrease with increasing H_2O content. If orthopyroxene was the liquidus phase for the Merensky Reef magma the addition of fluid (H_2O) to the magma could have caused orthopyroxene dissolution. This is illustrated by the phase change from A to B in Fig. 7. Chromite may also have been crystallized at this time, but because its stability is not suppressed by fluid addition as much as silicate minerals it continues to grow. Alternatively, the addition of fluid to the magma may have caused chromite crystallization.

The trapped orthopyroxene crystals in the composite mineral inclusions in the Merensky Reef chromites may

Table 3 Major element concentrations of bulk inclusion and selective magmas

Sample	SiO_2	TiO_2	Al_2O_3	Cr_2O_3	FeO^{total}	MnO	MgO	CaO	Na_2O	K_2O	Total
Bulk inclusion composition[a]	47.65	2.50	9.51	1.83	4.41	0.05	26.16	1.16	2.41	1.48	97.16
Basaltic andesite[b]	55.31	0.37	12.42	0.14	9.15	0.21	12.52	7.22	1.53	0.76	99.63
B3 magma[c]	50.70	0.41	16.03	0.03	9.14	0.17	9.21	11.14	2.52	0.23	99.58
Fractionated magma[d]	57.76	0.58	17.62	0.04	8.75	0.35	3.39	7.71	2.41	1.29	99.90
Merensky Reef magma[e]	54.23	0.50	16.83	0.04	8.95	0.26	6.30	9.43	2.46	0.76	99.74

[a] Also contains 2.6 wt% H_2O, 0.11 wt% F and 0.06 wt% Cl

[b] Average composition of chilled marginal rocks of the Lower Zone of the Bushveld Complex (Harmer and Sharpe 1985)

[c] Average B3 magma of Sharpe (1981) proposed as parental to the Main Zone of the Bushveld Complex

[d] Residual liquid of the basaltic andesite with 1 wt% H_2O after plagioclase appears on the liquidus (44% crystallization), Calculated using the MELTS program of Ghiorso and Sack (1995) under 2 kb and QFM buffer

[e] mixture of the fractionated magma and the B3 magma (50:50)

Table 4 δ^{18}O values (‰, V-SMOW) of minerals from the Merensky Reef on the farm Vlakforntein

Depth (m)	Orthopyroxene	Plagioclase	Phlogopite	Chromite	Inclusion-rich chromite
1675.9	6.6	6.8			
1676.46	6.8	7.0	6.0		
1676.65	7.0	7.1	6.5		
1676.79	6.9	6.9	6.3		
1676.9	6.5		6.0		
1676.91	6.1		5.8		
1676.93	6.7		5.9		
1676.94	7.3				
1676.96	6.3		6.3		
1676.97	6.2				
1676.98	6.9		6.8		
1676.99	6.8		6.4		
1677	6.3				
1677.01				4.6	5.9
1677.015				4.3	5.3
1677.02				4.7	6.1
1677.025				4.8	5.4
1677.03	7.2	7.4		4.3	
1677.06		7.0			

represent residual crystals from partial dissolution by hydrated magma. The trapped melts may represent mixtures of an orthopyroxene partial melt, the Merensky Reef magma and possibly a fluid phase. Variation in the proportions of these components during the mixing process would result in variation in the bulk composition of the trapped orthopyroxene crystals plus melt.

The absence of Na-phlogopite in the matrix of the chromitite seam is thought to be a function of essentially closed system trapping of the volatile-rich melt. As the melt in the interstices of the accumulating chromite grains crystallized, fluid saturation would be reached and a magmatic vapor could again rise to higher levels in the intrusive system. There is ample evidence for the trapping of saline fluid inclusions in late stage quartz in the Merensky Reef (Ballhaus and Stumpfl 1986). In contrast to an open system process, the volatile-rich melt trapped in the growing chromite could not liberate a fluid as it crysallized. The result of the process was the formation of Na- and K-phlogopite, and local conversion of pyroxene to amphibole.

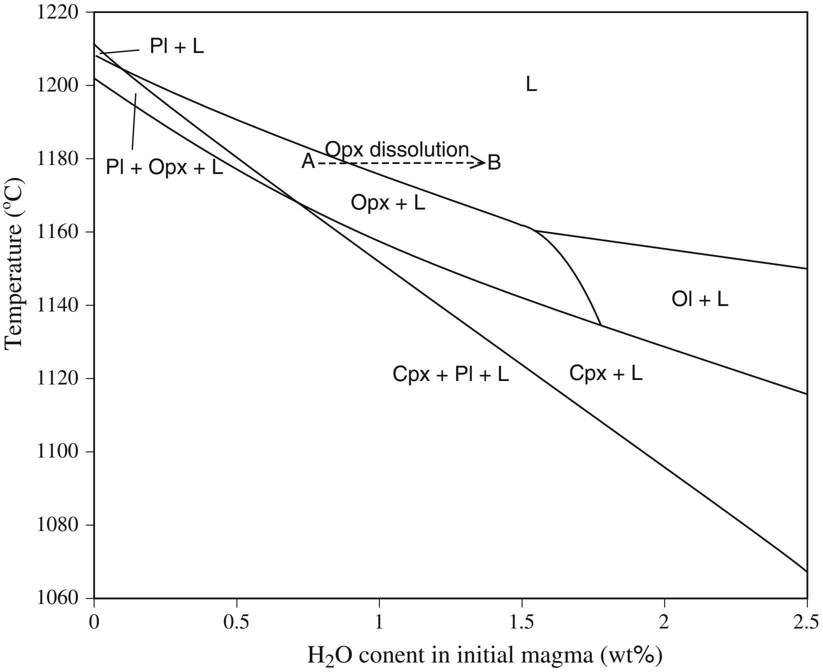

Fig. 7 Phase equilibria of a possible parental magma to the Merensky Reef with variable H_2O contents at 2 kb total pressure and QFM-buffer, calculated using the MELTS program of Ghiorso and Sack (1995). See text for discussions

Origin of the fluid

Plagioclase-orthopyroxene and orthopyroxene-chromite Δ values suggest equilibration temperatures near 1,200°C using the fractionation factors of Zheng (1991, 1993). Orthopyroxene-phlogopite Δ values are slightly higher than expected using the fractionation factors of Rosenbaum et al. (1994) and Valley (2003), but consistent with a high temperature exchange process. None of the minerals in the Merensky Reef exhibit oxygen isotopic values that are suggestive of low-temperature exchange with a non-magmatic fluid. The oxygen isotopic values of silicate minerals and chromite, as well as the hydrogen isotopic composition of hydrous minerals included within chromite, are consistent with a model of magmatic fluid deviation from underlying crystal pile as proposed by Nicholson and Mathez (1991).

Conclusions

Composite mineral inclusions found in chromite from the Merensky Reef provide additional evidence for the involvement of a fluid phase during formation of the reef rocks. The high concentration of Na_2O, K_2O and H_2O in the inclusions suggests addition of a Na-K rich fluid to the melt during chromite crystallization on the floor of the magma chamber. The addition of the fluid to the magma caused the dissolution of orthopyroxene. The trapping of small residual orthopyroxene crystals, along with the volatile-rich melt, led to the formation of the orthopyroxene-phlogopite dominant assemblages. Oxygen and hydrogen isotopic data are consistent with the premise that the fluid was of magmatic origin, and derived from the underlying crystal pile. The composite inclusions found in chromite support the mineralogical and isotopic data of Nicholson and Mathez (1991), Mathez et al. (1994), and Mathez (1995), and the fluid inclusion evidence of Ballhaus and Stumpfl (1986) for the involvement of fluids in the formation of the Merensky Reef of the Bushveld Complex.

Acknowledgements We thank Alan Boudreau and Edmond Mathez for their thoughtful reviews of the manuscript. Partial financial support for this study was provided through NSF grant EAR0335131 to EMR and CL, and through a Korean PDF fellowship to DS.

References

Ballhaus CG, Stumpfl EF (1986) Sulfide and platinum mineralization in the Merensky Reef: evidence from hydrous silicates and fluid inclusions. Contrib Mineral Petrol 94:193–204

Barnes S-J, Maier WD (2002) Platinum-group elements and microstructures of normal Merensky Reef from Impala Platinum Mines, Bushveld Complex. J Petrol 43:103–128

Boudreau AE (1988) Investigation of the Stillwater Complex IV The role of volatiles in the petrogenesis of the J-M Reef, Minneapolis adit section. Can Mineral 26:193–208

Boudreau AE, Mathez EA, McCallum IS (1986) Halogen geochemistry of the Stillwater and Bushveld Complexes: evidence for the transport of the platinum-group elements by Cl-rich fluids. J Petrol 27:967–986

Cameron EN (1979) Titanium bearing oxide minerals of the critical zone of the Eastern Bushveld. Am Mineral 64:140–150

Carman JH (1974) Synthetic sodium phlogopite and its two hydrates. Am Mineral 59:261–273

Cawthorn RG, Merkle RKW, Viljoen MJ (2002) Platinum-group element deposits in the Bushveld Complex, South Africa. In: Cabri LJ (ed) The Geology, Geochemistry, Mineralogy, and Mineral Beneficiation of Platinum-group Elements. Canadian Institute of Mining, Metallurgy and Petroleum Special vol 54:389–429

Clayton RN, Mayeda TK (1963) The use of bromine pentafluoride in the extraction of oxygen from oxides and silicates for isotopic analysis. Geochim Cosmochim Acta 27:43–52

Deer WA, Howie RA, Zussman J (1992) An introduction to the rock-forming minerals 2nd edn. Longman, England, pp 696

Eales HV, Cawthorn RG (1996) The Bushveld Complex. In: Cawthorn RG (ed) Layered Intrusions. Elsevier, Amsterdam, pp 181–229

Eiler JM (2001) Oxygen isotope variations of basaltic lavas and upper mantle rocks. Rev Mineral 43:319–364

Ford CE, Biggar GM, Humphries DJ, Wilson G, Dixon D, O'Hara MJ (1972) Role of water in the evolution of lunar crust: an experimental study of sample 14310; an indication of lunar calc-alkaline volcanism. In: Proceedings of 3rd Lunar Science conference, pp 207–229

Gaetani GA, Grove TL, Bryan WB (1994) Experimental phase relations of basaltic andesite from hole 839B under hydrous and anhydrous conditions. Proc Ocean Drill Prog Sci Rep 135:557–563

Ghiorso MS, Sack RO (1995) Chemical mass transfer in magmatic processes IV A revised and internally consistent thermodynamic model for the interpolation and extrapolation of liquid-solid equilibria in magmatic systems at elevated temperature and pressure. Contrib Mineral Petrol 119:197–212

Hall AL (1932) The Bushveld Complex in the central Transvaal. Geol Soc South Africa Memoir 28:544

Harmer RE, Sharpe MR (1985) Field relations and strontium isotope systematic of the marginal rocks of the eastern Bushveld Complex. Econ Geol 80:813–837

Harris C, Pronost JJ, Ashwal LD, Cawthorn RG, (2004) Oxygen and hydrogen isotope stratigraphy of the Rustenburg layered suite, Bushveld Complex: constraints on crustal contamination. J Petrol 46:579–601

Hiemstra SA (1986) The distribution of chalcophile and platinum-group elements in the UG2 chromitite layer of the Bushveld Complex. Econ Geol 81:1080–1086

Hulbert LJ, von Gruenewaldt G (1985) Textural and compositional features of chromite in the lower and critical zones of the Bushveld Complex south of Potgietersrus. Econ Geol 80:872–895

Irvine TN (1975) Crystallization sequences in the Muskox intrusion and other layered intrusions—II. Origin of chromitite layers and similar deposits of other magmatic ores. Geochim Cosmochim Acta 39:991–1020

Irvine TN (1977) Chromite crystallization in the join Mg_2SiO_4-$CaMgSi_2O_6$-$CaAl_2Si_2O_8$-$MgCr_2O_4$-SiO_2. Carnegie Institute of Washington Year Book 76:465–472

Irvine TN, Sharpe MR (1986) Magma mixing and the origin of stratiform oxide ore layers in the Bushveld and Stillwater Complexes. In: Gallagher MJ, Ixer R, Neary CR, Prichard HM (eds) Metallogeny of basic and ultrabasic rocks. Institution of Mining and Metallurgy, London, pp 183–198

Ito E, White WM, Gopel C (1987) The O, Sr, Nd, and Pb isotope geochemistry of MORB. Chem Geol 62:157–176

Kingston GA, El-Dosuky BT (1982) A contribution on the platinum-group mineralogy of the Merensky Reef at the Rustenburg Platinum Mine. Econ Geol 77:1367–1384

Kroger FJ, Kinnaird JA, Nex PAM, Cawthorn GR (2002) Chromite is the key to PGE. In: 9th International Platinum Symposium. Abstract and Program, 21–25 July 2002, Billings, Montana, pp 211–213

Kruger FJ, Marsh JS (1982) The significance of ^{87} Sr/^{86} Sr ratios in the Merensky cyclic unit of the Bushveld Complex. Nature 298:53–55

Lee CA (1983) Trace and platinum-group element geochemistry and the development of the Merensky unit of the western Bushveld Complex. Miner Deposita 18:173–190

Leeb-du Toit A (1986) The Impala Platinum mines. In: Anhaeusser CR, Maske S (eds) Mineral Deposits of South Africa. Geol Soc South Africa, Johannesburg, pp 1091–1106

Legg CA (1969) Some chromite-ilmenite association in the Merensky Reef, Transvaal. Am Mineral 54:1347–1354

Li C, Ripley EM, Merino M, Maier WD (2004) Replacement of base metal sulfides by actinolite, epidote, calcite and magnetite in the UG2 and Merensky Reef of the Bushveld Complex, South Africa. Econ Geol 99:173–184

Lorand JP, Ceuleneen (1989) Silicate and base-metal sulfide inclusions in chromites from the Maqsad area (Oman ophiolite, Gulf of Oman): a model for entrapment. Lithos 22:173–190

Lorand JP, Cottin JY (1987) Na-Ti-Zr-H_2O-rich mineral inclusions indicating postcumulus chrome-spinel dissolution and recrystallization in the Western Laouni mafic intrusion, Algeria. Contrib Mineral Petrol 97:251–263

Luth WC (1967) Studies in the system $KAlSiO_4$-Mg_2SiO_4-SiO_2-H_2O, I Inferred phase relations and petrologic implications. J Petrol 8:372–416

MacNeil AM, Edgar AD (1987) Sodium-rich metasomatism in the upper mantle: implications of experiments on the pyrolite-Na_2O-rich fluid system at 950°C, 20 kbar. Geochim Cosmochim Acta 51:2285–2294

Maier WD, Barnes S-J (1998) Concentrations of rare earth elements in silicate rocks of the Lower, Critical and Main Zones of the Bushveld Complex. Chem Geol 150:85–103

Maier WD, Arndt NT, Curl E (2000) Progressive crustal contamination of the Bushveld Complex: evidence from Nd isotopic analyses of the cumulus rocks. Contrib Mineral Petrol 140:328–343

Mathez EA (1995) Magmatic metasomatism and formation of the Merensky reef, Bushveld Complex. Contrib Mineral Petrol 119:227–286

Mathez EA, Webster JD (2004) Partitioning behavior of chlorine and flurine in the system apatitite-silicate melt-fluid. Geochim Cosmochim Acta 69:1275–1286

Mathez EA, Agrinier P, Hutchinson R (1994) Hydrogen isotopic composition of the Merensky Reef and related rocks, Atok section, Bushveld Cmplex. Econ Geol 89:791–802

Mathez EA, Hunter RH, Kinzler R (1997) Petrologic evolution of partially molten cumulate: the Atok section of the Bushveld Complex. Contrib Mineral Petrol 129:20–40

McDonald JA (1965) Liquid immiscibility as a factor in chromite seam formation in the Bushveld igneous complex. Econ Geol 60:1674–1685

Mostert AB, Hofmeyr PK, Potgieter GA (1982) The platinum-group mineralogy of the Merensky Reef at the Impala Platinum Mines, Bophuthatswana. Econ Geol 77:1385–1394

Nicholson DM, Mathez EA (1991) Petrogenesis of the Merensky Reef in the Rustenburg section of the Bushveld Complex. Contrib Mineral Petrol 107:293–309

Prichard HM, Barnes S-J, Maier WD, Fisher PC (2004) Variations of in the nature of platinum-group minerals in a cross section through the Merensky Reef at Impala Platinum: implications for the mode of formation of the Reef. Can Mineral 42:423–437

Prior DJ, Boyle AP, Brenker F, Cheadle MC, Day A, Lopez G, Peruzzo L, Potts GJ, Reddy S, Spiess R, Timms NE, Trimby P, Wheeler J, Zetterström L (1999) The application of electron backscatter diffraction and orientation imaging in the SEM to textural problems in rocks. Am Mineral 84:1741–1759

Rosenbaum JM, Kyser TK, Walker D (1994) High temperature oxygen isotope fractionation in the enstatite-olivine-$BaCO_3$ system. Geochim Cosmochim Acta 58:2653–2660

Schiffries CM, Rye DM (1989) Stable isotopic systematics of the Bushveld Complex: I. Constraints of magmatic processes in layered intrusions. Am J Sci 289:841–873

Sharp ZD, Atudorei V, Durakiewiez T (2001) A rapid method for determination of hydrogen and oxygen isotope ratio from water and hydrous minerals. Chem Geol 173:197–210

Sharpe MR (1981) The chronology of magma influxes to the eastern compartment of the Bushveld Complex as exemplified by its marginal border groups. J Geol Soc London 138:307–326

Sisson TW, Grove TL (1993) Experimental investigations of the role of H_2O in cal-alkaline differentiation and subduction zone magmatism. Contrib Mineral Petrol 113:143–166

Stumpfl EF, Rucklidge JC (1982) The platiniferous dunite pipes of the eastern Bushveld. Econ Geol 77:1419–1431

Valley JW (2003) Oxygen isotopes in zircon. In: Hanchar JM, Hoskin PWO (eds) Zircon. Rev Mineral Geochem 53:343–385

Viljoen MJ, Hieber R (1986) The Rostenburg Section of Rustenburg Platinum Mines Limited, with reference to the Merensky Reef. In: Anhaeusser CR, Maske S (eds) Mineral deposits of South Africa. Geological Society of South Africa, Johannesburg, pp 1107–1134

Willmore CC, Boudreau AE, Kruger FJ (2000) The halogen geochemistry of the Bushveld Complex: Republic of South Africa: implications for chalcophile element distribution in the lower and critical zones. J Petrol 41:1517–1539

Zheng Y-F (1991) Calculation of oxygen isotope fractionation in metal oxides. Geochim Cosmochim Acta 55:2299–2307

Zheng Y-F (1993) Calculation of oxygen isotope fractionation in anhydrous silicate minerals. Geochim Cosmochim Acta 57:1079–1091